24th COBEM - 2017

24th ABCM International Congress of Mechanical Engineering
December 3-8, 2017, Curitiba, PR, Brazil

# COBEM-2017-2631
# A COMPARATIVE ANALYSIS OF THE THERMAL PERFORMANCE OF THE REFRIGERANTS R134A, R245FA, R407C AND R600A DURING FLOW BOILING IN A MICROCHANNELS HEAT SINK

**Hugo Leonardo Souza Lara Leão**[1,2]
**Gherhardt Ribatski**[1]
[1] Heat Transfer Research Group, Escola de Engenharia de São Carlos, EESC - University of São Paulo (USP), São Carlos, Brazil
[2] Instituto Federal Goiano campus Rio Verde, Rio Verde, Brazil
Emails: hugoleao@ifgoiano.edu.br; ribatski@sc.usp.br

***Abstract.*** *The present paper concerns a comparative study of the performances of the refrigerants R134a, R407C, R245fa and R600a during flow boiling in a 123x494 μm² microchannels heat sink composed of 50 parallel rectangular channels. Experimental results for the heat transfer coefficient were obtained for footprint heat fluxes up to 310 kW m$^{-2}$, mass velocities from 400 to 1000 kg m$^{-2}$ s$^{-1}$, liquid subcoolings at the test section inlet of 5 and 10 °C and saturation temperatures about 30ºC for R245fa and 26 °C for R134a, R407C and R600a. The experimental results for the refrigerants R134a, R407C and R245fa were extracted from previous studies performed by the group. From the analyses of the database, average effective heat transfer coefficients up to 10 kW m$^{-2}$ °C$^{-1}$ were found. The onset of nucleate boiling (ONB) was identified, in particular, the fluids R245fa and R407C presented the highest and lowest superheating necessary to trigger the boiling process, respectively. The refrigerants R600a and R407C presented the highest and the lowest heat transfer coefficients, respectively.*

***Keywords:*** *Flow Boiling, Heat Transfer Coefficient, Microchannels Heat sink*

## 1. INTRODUCTION

Over the last decades, the size of electronic devices decreased substantially, as result of the increase of the number of transistors in a microprocessor that was possible due to the evolution of manufacturing techniques. However, the progressive miniaturization of chips was followed by an increasing demand of dissipating heat. In this context, the electronic industry is facing the challenge of removing heat fluxes up to 300 W cm$^{-2}$. Moreover, according to Agostini et al. (2007) and do Nascimento et al. (2013), the need of dissipating even higher heat fluxes is expected for a near future. In general, forced-convection of a liquid through microchannels, especially water, is being implemented for replacing air-cooling, as a more efficient solution (Colgan et al., 2007; Tuckerman and Pease, 1981). Besides, heat spreaders based on flow boiling mechanism through microchannels are being also considered as an alternative for thermal management of microprocessors. As advantages over single-phase based cooling, evaporation process provides higher heat transfer coefficients and almost isothermal temperature distribution along the surface of the heat spreader. These characteristics favor the compactness of the heat spreader and the improvement of the microprocessor performance. It is important highlighting that the need of dissipating extremely high heat fluxes under conditions of well-conditioned temperatures is also observed in laser diodes, microchemical reactors, solar power concentrators, nuclear power plants, accelerators of particles, medical equipment, lens and mirrors.

According to the broad literature review performed by Sempértegui-Tapia and Ribatski (2013), most of studies concerning flow boiling through heat sinks based on multi- microchannels were performed for parallel channels with rectangular cross sections. Most of these heat sinks were fabricated in silicon and copper, due to the high thermal conductivity of these materials.

Due to their contribution to ozone layer depletion and greenhouse effect, CFCs, HCFCs and HFCs are being discarded as refrigerant and various alternatives were proposed and evaluated to replace them, as hydrofluoroolefins (HFOs) and natural refrigerants (hydrocarbons, $CO_2$ and ammonia). As pointed out by Thome (1996) and Chen et al. (2005), despite of some concerns about flammable refrigerants due to safety aspects, propane and isobutene are widely used as refrigerants in applications involving cascade refrigeration systems in ethylene production facilities and new domestic refrigerators. In this context, it is important to highlight the almost negligible refrigerant charge contained in a heat spreader developed for electronic cooling, corresponding, for the configuration evaluated in the present study, to

only 0.16 g assuming all the channels filled with liquid and to 0.12 g under evaporation conditions. However, most of studies on flow boiling through heat spreaders based on microchannels were performed for halocarbon refrigerants and water as pointed out by Chávez et al. (2014).

The literature (Agostini and Thome, 2005; Harirchian and Garimella, 2009; Zhang, 2005) pointed out that the knowledge of the heat transfer coefficient during flow boiling in a microchannel-based heat spreader is still limited due to a complex combination of heat transfer and two-phase flow mechanisms. According to Tibiriçá and Ribatski (2013) and Agostini and Thome (2005), distinct heat transfer trends during flow boiling in microchannels occur when studies from different laboratories are compared. Additionally, the main heat transfer mechanisms during flow boiling inside microchannels are still unknown. Nevertheless, several experimental studies indicate that flow boiling heat transfer is governed by two important effects: nucleate boiling and forced convection, and several of these studies (Kaew-On and Wongwises, 2009; Kaew-On et al., 2011; Kew and Cornwell, 1997) have concluded that the nucleate boiling effects are predominant over forced convection effects for flow boiling in microchannels heat sinks.

Studies available in the open literature have highlighted the presence of thermal instabilities which are responsible for drastic reductions of the overall heat transfer coefficient (Bertsch et al., 2008; Chen and Garimella, 2006; Daniels et al., 2011; Hetsroni et al., 2002; Park and Thome, 2010; Wang et al., 2008; Xu et al., 2005). These instabilities affect not only the heat transfer coefficient but also enhances the pressure drop and diminishes the critical heat flux. Recently, Ribatski (2013) have emphasized that the flow pattern dynamics in multi-microchannels are not the same as in single microchannels. In multi-microchannels configurations, backflows are usually present. The inlet plenum configuration influences the two-phase flow topology and its dynamics along the channels, affecting, consequently, the heat transfer coefficient, pressure drop and critical heat flux.

Szczukiewicz et al. (2014) observed significant mal-distribution effects of the refrigerant among the channels and its harmful effect on the temperature distribution on the footprint surface of a heat sink based on parallel microchannels. By adding restrictions to the flow at the inlet of each microchannel, Szczukiewicz et al. (2014) equalized the two-phase flow distribution among the channels and minimized thermal instability effects. Analogous to Ribatski (2013), Szczukiewicz et al. (2014) also pointed out that care should be taken when experimental data for microchannels based heat sinks are compared with data and predictive methods for single-channels due to differences in the heat transfer and fluid dynamic behaviors.

In this context, the present study presents a comparison of heat transfer performance during flow boiling in a heat spreader based on multi-microchannel for refrigerants R600a R134a, R245fa and R407C. The refrigerant R600a is a medium pressure natural refrigerant that can be considered suitable to replace R134a and R407C. On the other hand, R245fa is a low-pressure refrigerant, and, therefore less suitable to leaks concerns. The experimental results cover heat fluxes up to 320 kW $m^{-2}$ (based on the footprint area) and average saturation temperatures referred to the pressure at the microchannels inlet of 31°C for R245fa and 26 °C for R600a R134a, and R407C. The experimental results are carefully analyzed.

## 2. EXPERIMENTAL APARATUS AND DATA REDUCTION

The test facility comprises a refrigerant closed loop, shown schematically in Fig. 1, and a secondary circuit, used to condense and cool down the test fluid at the refrigerant loop. Both circuits are well detailed by do Nascimento et al. (2013) and Leão et al. (2014, 2015). These references are suggested for those interested in a detailed and complete description of the test facility.

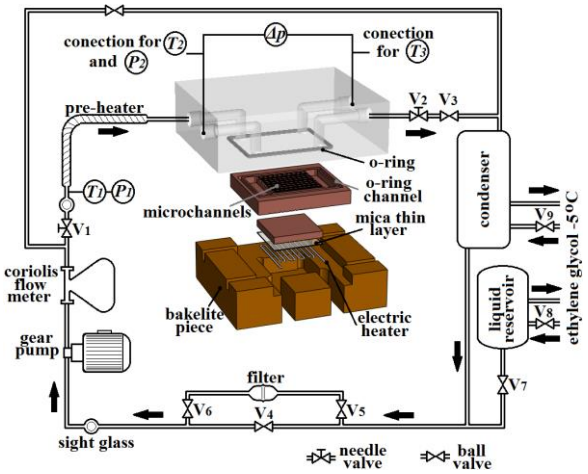


Figure 1. Schematic of the flow boiling test facility and test section. (Leão et al., 2015)

In the refrigerant circuit, the test fluid is driven by an oil-free gear micropump and the mass flow rate is measured by a Coriolis mass flow meter. A needle valve is installed in the circuit main line, upstream the pre-heater, to minimize the propagation of instability effects from the test section to remaining circuit and vice versa. A pre-heater consisting of a

copper tube of a diameter of 12.7 mm wrapped with tape-type electrical resistances is installed upstream of the test section to heat up the test fluid to the desired inlet subcooling temperature.

The test section, schematically illustrated in Figure 1, consists of a 28x25x4 $mm^3$ copper block containing fifty parallel microchannels with width, depth, and total length of 123.3, 494.2 μm and 15 mm, respectively. The distance between two consecutive microchannels is 176.9 μm. The surface roughness is 0.29 μm. The heat sink is covered with a transparent Pyrex cover plate of thickness of 15 mm.

The test fluid is supplied to the inlet plenum and drained from the outlet plenum of the heat sink by channels with internal diameters of 3.5 mm machined through the Pyrex cover plate. One additional pair of channels positioned over the inlet and outlet plenums were machined in the Pyrex plate. These additional channels were connected to the absolute and differential pressure transducers to measure the pressure at the test section inlet and the pressure drop along the test section. The same channels are also used to measure the bulk temperature at the inlet and outlet plenums.

On the backside of the heat sink, the wall temperature is measured through nine K-type thermocouples embedded within the heat sink wall and distributed according to a 3x3 matrix. A copper block was positioned between the electrical resistance and the heat sink to uniform the heat flux generated by the electrical resistance. The heating effect is obtained through a 0.5 Ω electrical resistance composed by a continuous Kanthal wire bent as a serpentine.

A second needle valve is installed downstream of the test section with the same purpose of the needle valve located upstream the test section. Then, a ball valve is installed for isolating the heat sink, allowing its maintenance without the need of evacuating the refrigerant circuit. Downstream the ball valve, the working fluid is condensate and subcooled in a plate-type heat exchanger by exchanging heat with the anti-freezing ethylene glycol aqueous solution from the secondary circuit. Downstream the plate-type heat exchanger, a pipeline connects the refrigerant tank and the refrigerant circuit. The refrigerant tank operates as a reservoir of the working fluid and is used to control the saturation pressure at the refrigerant circuit. Downstream of the refrigerant tank and parallel to the main pipeline is an alternative pipeline which has a filter-drier installed between two ball valves. By manipulating these valves, the test fluid is driven through the filter in order of removing particles dispersed in the refrigerant.

The electrical signals of the measurements were acquired, processed and stored by a National Instruments SCXI-1000 chassis that communicates with the LabView software. The database analyzed in the present study comprises experimental results for mass velocities from 300 to 800 kg $m^{-2}s^{-1}$, heat fluxes up to 320 kW $m^{-2}$ (based on the footprint area) and liquid subcooling at the test section inlet of 5 and 10 °C. Particularly in the present study, the results were obtained for the refrigerant R600a. The data for R134a, R407 and R245fa were obtained in the same test facility and were previously published by do Nascimento et al. (2013) and Leão et al. (2014, 2015).

The mas velocity, G, is given as the ratio between the mass flow rate, $\dot{m}$, measured by the Coriolis flow meter, and fifty times the cross-sectional area of one single channel, so, assuming uniform mass flow distribution among the channels. Although neglected in the data reduction procedure, fluid maldistribution and flow instabilities causing reverse flow were observed during the experiments. However, measuring the flow rate and heat flux along each channel is not feasible. Moreover, the present paper concerns a comparative evaluation of the overall performance of the heat sink, what makes the present data regression procedure appropriate.

The amount of heat transferred to the fluid in the region of the heat sink containing the microchannels, $\dot{Q}_{real}$, is given as the electrical power supplied to the Kanthal resistance in the test section, $\dot{Q}_{elet}$, minus the heat losses to the environment, $\dot{Q}_{env}$, and the heat transferred to the fluid at the inlet and outlet plenums, $\dot{Q}_{in,plm}$ and $\dot{Q}_{out,plm}$. Heat losses to the environment, $\dot{Q}_{env}$, were evaluated from energy balances for single-phase flow tests. These energy balances are based on comparisons of the electrical power supplied to the heat sink and the product between the mass flow rate and the variation of enthalpy of the refrigerant between the inlet and outlet of the heat sink. This analysis reveals average heat losses to the environment ranging from 16 to 18% of the total electrical energy supplied to the heat sink. The heat transferred to the fluid in the regions of the plenums, $\dot{Q}_{in,plm}$, and $\dot{Q}_{out,plm}$, was estimated based on the superficial area of the plenums contacting the fluid, the local temperature of the refrigerant and the average temperature of the heat-sink, $\overline{T}_{wall}$, evaluated based on the measurements of the thermocouples embedded within the heat sink wall. For this purpose, the heat transfer correlations of Stephan and Preußer (1979) and Li and Wu (2010) were used for single-phase and flow boiling conditions, respectively. In these analyses, it was assumed that heat is transferred only through the copper surface of the heat sink contacting the test fluid.

The effective heat flux, $q''_{eff}$, was defined as the ratio between $\dot{Q}_{real}$ and the heated area of the microchannels contacting the fluid given as the product of the heated perimeter, the channels length and the number of channels.

The average wall superheating of the heat sink, $\Delta\overline{T}$, was calculated as the difference between the average temperature of the heat sink wall, $\overline{T}_{wall}$, and the average temperature of the refrigerant along the microchannels length, $\overline{T}_{fluid}$. The average temperature of the test fluid along the microchannels was estimated considering a uniform heat flux along the channel surface and considering the lengths of the subcooled and saturated regions, assumed as single- and two-phase flow regions, respectively. The temperature at the end of the single-phase region, $T_{end,1\phi}$, and the single-phase pressure drop over this length were estimated based on the heat flux and the measured temperature and pressure at the inlet plenum of the heat sink by solving simultaneously an equation of state relating $p_{sat}$ and $T_{sat}$ plus energy balance and single-phase pressure drop equations. To estimate the temperature profile along the flow boiling region, the length of the microchannels corresponding to two-phase flow was discretized and for each element the local pressure and vapor quality were determined based on energy balance over each discrete element and the corresponding pressure drop calculated according to the Homogenous model, with the two-phase dynamic viscosity given by the Maxwell Eucken 2 model (Awad and Muzychka, 2008; Levy, 1981) that provided good prediction of the pressure drop experimental data.

The entrance and exit pressure drops due the contraction and expansion at the inlet and outlet plenums, the single-phase and acceleracional pressure drops were also considered. For single-phase flow experiments along all the channels, the fluid temperature was given as the average temperature between measurements at the inlet and outlet plenums.

Average heat transfer coefficients were estimated through the Newton's cooling law according to the following approaches: (i) based on the effective heat transfer coefficient, $\bar{h}_{eff}$ corresponding to the overall heat transfer coefficient of the heat sink. These heat transfer coefficient data were considered to evaluate the overall heat transfer performance of the heat sink for the different fluids; (ii) based on the two-phase heat transfer coefficient, $\bar{h}_{TP}$, considers only the region of the heat sink estimated as being under flow boiling conditions. The data for $\bar{h}_{TP}$ were considered for the comparisons with predictive methods from literature. The definitions of the heat transfer coefficients are given as follows:

$$\bar{h}_{eff} = q''_{eff} \big/ \Delta\bar{T} \tag{1}$$

$$\bar{h}_{TP} = q''_{eff} \big/ \Delta\bar{T}_{TP} \tag{2}$$

where $\Delta\bar{T}_{TP}$ is the average wall superheating over the two-phase flow region of the heat sink, calculated as the difference between the average heat-sink wall temperature and the average temperature of the fluid over the two-phase flow region.

The average vapor quality over the heat sink, $\bar{x}$, was determined as the arithmetic average value of the thermodynamic vapor qualities at the inlet and outlet plenums. The average vapor quality over the two-phase region, $\bar{x}_0$, was defined as the arithmetic average value of the thermodynamic vapor qualities at the outlet plenum and at the onset of two-phase flow, corresponding to a thermodynamic vapor quality assumed equal to zero.

Table 1. Uncertainties of measured and calculated parameters.

| **Parameters** | **Uncertainty** | **Parameters** | **Uncertainty** |
|---|---|---|---|
| H [μm] | 22.9 | $\Delta\bar{T}$ [°C] | 0.45 |
| W [μm] | 15.4 | $\Delta T_{sub}$ | 0.3 |
| L [μm] | 5 | p [kPa] | 2 |
| G [kg m$^{-2}$ s$^{-1}$] | 132 | Δp [kPa] | 0.2 |
| T [°C] | 0.15 | q″ [kW m$^{-2}$] | 0.8 |
| $\bar{T}_{wall}$ [°C] | 0.4 | $\bar{h}$ [kW m$^{-2}$ °C$^{-1}$] | 1.3 |
| $\bar{T}_{fluid}$ [°C] | 0.2 | | |

The experimental data presented in this paper were obtained by gradually increasing from a null value the heat flux until a maximum and then decreasing its value down to zero. Temperature measurements were calibrated and their uncertainties were evaluated according to the procedure proposed by Abernethy and Thompson (1973). For the remaining sensors and measuring devices, the uncertainties were assumed equal to the specifications provided by the manufacturers. Accounting for all instrument errors, uncertainties for the calculated parameter were estimated according to the method of sequential perturbation by Moffat (1988) that considers that any measure $X_i$ presents a $\delta X_i$ uncertainty. The experimental uncertainties associated with the sensors and calculated parameters are presented in Table 1.

For those interested on a detailed description of the data regression procedure, the previous paper by Leão et al. (2015) is recommended as reference.

## 3. EXPERIMENTAL RESULTS

The experimental apparatus and the data regression procedures were validated by comparing single-phase flow data against predictions from well-established correlations from literature for pressure drop and heat transfer coefficient. The validation data were obtained for R245fa as presented by Leão et al. (2015). The method of Shah and London (1978) for rectangular channels and laminar flow captured reasonably well the experimental trends for the frictional pressure drop, and the method of Stephan and Preußer (1979) for laminar flow, uniform heat flux, simultaneous developing flow and circular ducts also captured reasonably well the trends of the experimental results for heat transfer coefficient.

Table 2 compares the thermophysical properties of the refrigerants evaluated in the present study. According to this table, in general, the refrigerant R600a presents the best characteristics, as the highest thermal conductivity and the specific heat contributing for the enhancement of the convective effects. The refrigerant R600a possess also advantages over the other fluids from an environmental point of view because its ODP is null and its GWP is only 3. The concerns of using R600a is its high flammability that is not crucial considering the reduced fluid amount used in such an application, as shown in Tab. 2.

Table 2. Thermophysical properties of the refrigerants.

| **Properties** | **R407C** | **R134a** | **R600a** | **R245fa** |
|---|---|---|---|---|
| Critical pressure [kPa] | 4632 | 4059 | 3640 | 3651 |
| Critical temperature [°C] | 86.2 | 101 | 134.7 | 154 |
| Liquid saturated pressure at 25 °C [kPa] | 1190 | 665.8 | 350.4 | 147.8 |
| Liquid density at 25 °C [kg $m^{-3}$] | 1138 | 1207 | 549.9 | 1339 |
| Vapor density at 25 °C [kg $m^{-3}$] | 43.72 | 32.37 | 9.123 | 8.525 |
| Liquid viscosity at 25 °C [kg $m^{-1}$ $s^{-1}$] | 0.0001516 | 0.0001944 | 0.00015 | 0.0004063 |
| Vapor viscosity at 25 °C [kg $m^{-1}$ $s^{-1}$] | 0.00001261 | 0.00001197 | 0.000007739 | 0.0001015 |
| Liquid specific heat at 25 °C [kJ $kg^{-1}$ $°C^{-1}$] | 1.533 | 1.425 | 2.45 | 1.322 |
| Vapor specific heat at 25 °C [kJ $kg^{-1}$ $°C^{-1}$] | 1.133 | 1.032 | 1.819 | 0.9538 |
| Liquid thermal conductivity at 25 °C [W $m^{-1}$ $°C^{-1}$] | 0.0843 | 0.08323 | 0.08894 | 0.08115 |
| Vapor thermal conductivity at 25 °C [W $m^{-1}$ $°C^{-1}$] | 0.01442 | 0.01456 | 0.01694 | 0.01395 |
| Superficial tension [N $m^{-1}$] | 0.006892 | 0.008028 | 0.009857 | 0.01363 |
| Heat sink refrigerant inventory for liquid [mg]* | 340.1 | 359.6 | 163.2 | 396.8 |
| Heat sink refrigerant inventory for vapor [mg]* | 11 | 8.16 | 2.3 | 2.1 |
| Heat sink refrigerant inventory for liquid-vapor [mg]** | 269.6 | 281.8 | 126.7 | 299.8 |
| Inflamability | Non-flammable gas | Non-flammable gas | Flammable gas | Non-flammable gas |
| GWP (Global Warming Potential) | 1610 | 1300 | 3 | 1030 |
| ODP (Ozone Depletion Potential) | 0 | 0 | 0 | 0 |

* Conditions: $T_{sat}$=25 [°C]; ** Conditions: $T_{sat}$=25 [°C], G=400 [kg $m^{-2}$ $s^{-1}$], $\dot{Q}$=64 [W]

Figure 2 displays a comparison of boiling curves of the refrigerants R134a (do Nascimento et al., 2013), R407C (Leão et al., 2014), R245fa (Leão et al., 2015) and R600a for mass velocity of 400 kg $m^{-2}$ $s^{-1}$ and degrees of subcooling at the inlet plenum of 5 °C. According to this figure, initially the heat flux increases almost linearly with increasing the wall superheating. Then, the curves display discontinuities that result from a transition from a condition of only single-phase flow along all the channels to a condition with the presence of flow boiling. This phenomenon, named in literature as the onset of nucleate boiling (ONB), is related to the fact that an excess of superheating is necessary to trigger the boiling process. For results obtained by decreasing gradually the heat flux, as shown in Fig. 2, the nucleation sites are already active and, therefore, an excess of superheating is not necessary. This behavior implies that the boiling curves for increasing and decreasing heat flux do not follow the same path.

During the experimental campaign, care was exercised to identity the onset of nucleate boiling (ONB) corresponding to the superheating excess necessary to trigger the boiling process. So, before running the experiments and obtaining the data corresponding each boiling curve, the refrigerant inside the test section was maintained during 72 hours as quiescent liquid without heating. Such a procedure was adopted to deactivate the cavities and eliminate vapor nucleus on the heat sink surface that would favor an earlier ONB.

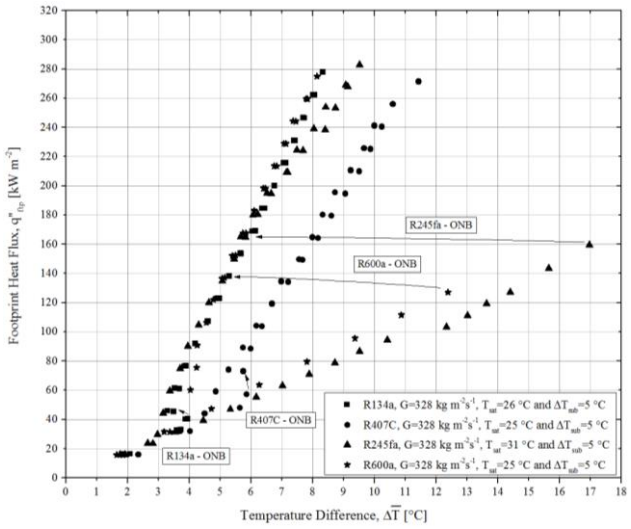


Figure 2. Boiling curves of refrigerants R134a, R407C, R245fa R600a for liquid subcooling at the inlet plenum of 5 °C and mass velocity of 328 kg $m^{-2}$ $s^{-1}$.

According to Fig. 2, the fluid R407C presents the lowest excess of superheating, followed by the refrigerants R134a, R600a and R245fa. Values higher than 12 °C can be noted in Fig. 2 for the refrigerant R245fa. As shown in Tab. 2, the

refrigerants R245fa and R600a present lower vapor density and higher surface tension than the refrigerants R407C and R134a. Therefore, the refrigerants R245fa and R600a require higher wall superheating to activate the cavities. High wall superheating to achieve the ONB is not desirable because this can lead either to a premature surface dryout or to a wall temperature higher than the safe value for the electronic device. This scenario becomes critical during startups of electronic devices, characterized by the absence of active nucleate boiling sites along the wet surface of the heat sink.

Bergles and Rohsenow (1964), Davis and Anderson (1966) and Kandlikar et al. (2006), just to mention a few authors, proposed criteria for determining the minimum wall superheating necessary to the onset of nucleate boiling. Kandlikar et al. (2006) proposed a criterion to predict the ONB giving by the following equation:

$$\Delta T_{sub,ONB} = \frac{q''}{\bar{h}} - \Delta T_{sat,ONB} = \frac{q''}{\bar{h}} - \sqrt{\frac{8.8 \cdot \sigma \cdot T_{sat} \cdot q''}{\rho_v \cdot i_{lv} \cdot k_l}} \tag{3}$$

Table 3 presents a comparison of the result for the ONB for R134a, R245fa, R407C and R600a. The ONB is higher for R245fa followed by R600a, R134a and R407C. This table illustrates a comparison between experimental data for the ONB obtained in the present study and the corresponding predictions given by the method of Kandlikar et al. (2006). According to this table, the method of Kandlikar et al. (2006) provides reasonable predictions of the experimental data. In general, the method under predicted the data with an error lower than 20 %, independently of the fluid.

Table 3. Comparison of experimental results and the predictions given by the method of Kandlikar et al. (2006) for the Onset of Nucleated Boiling under subcooled flow boiling conditions.

| Fluid | h [W m$^{-2}$ K$^{-1}$] | Heat flux [W m$^{-2}$] | $T_{sat}$ [K] | $\Delta T_{sub,ONB}$ calculated [K] | $\Delta T_{sub,ONB}$ experimental [K] | Mean Absolute Error, η [%] |
|---|---|---|---|---|---|---|
| R134a | 2363 | 8822 | 298.6 | 3.1 | 3.7 | 17% |
| R407C | 2295 | 12936 | 298.3 | 5.0 | 5.6 | 11% |
| R245fa | 2534 | 42990 | 303.3 | 13.7 | 17.0 | 19% |
| R600a | 2770 | 34299 | 298.2 | 10.6 | 12.4 | 14% |

Figure 3 displays the effects of the mass velocity and the degree of liquid subcooling at the microchannels inlet on the variation of the average effective heat transfer coefficient with increasing the average thermodynamic vapor quality for the refrigerant R600a. Experimental data corresponding single-phase flow conditions along the heat spreader are highlighted by circles containing the symbols corresponding to the data points. Under conditions of single-phase flow, Fig. 3A shows that, the effect of the variation of liquid subcooling on $\bar{h}_{eff}$ is almost negligible due to marginal changes of the transport properties with increasing fluid temperature at the inlet plenum. According to Fig. 3A, for a fixed value of $\bar{x}$ and under conditions of nucleate boiling and low average vapor qualities, the average effective heat transfer coefficient increases with increasing the liquid subcooling. However, the effect of liquid subcooling on $\bar{h}_{eff}$ decreases with increasing the average vapor quality until a certain value of $\bar{x}$ from which its effect on $\bar{h}_{eff}$ becomes negligible. Collier and Thome (1994) pointed out that the condition characterized by the ratio of heat flux and surface temperature independent of the liquid subcooling corresponds to fully developed subcooled boiling. Under this condition, the increment of heat flux implies on the increment of the surface temperature with the contribution of single-phase forced convection to the heat transfer rate becoming relatively negligible. For fully developed subcooled boiling, the whole surface is covered with nucleation sites and the vapor is generated in the form of isolated bubbles at preferred nucleation sites. Such behaviors were already pointed out in the previous studies for refrigerants R134a, R407C and R245fa (do Nascimento et al., 2013; Leão et al., 2015, 2014).

Figure 3B illustrates the effect of the mass velocity on the average effective heat transfer coefficient. According to this Figure, $\bar{h}_{eff}$ increases with increasing mass velocity. For only single-phase flow along the channels, this behavior was expected and agreed with the predictions given by the method of Stephan and Preußer (1979) for laminar flow, uniform heat flux and simultaneous developing flow region. Under the presence of flow boiling along the channels, the fact that the average effective heat transfer coefficient increases with increasing mass velocity seems related to the augmentation of heat flux to maintain $\bar{x}$ with increasing the mass velocity. This hypothesis is presented based on the work of Kanizawa et al. (2016) according to which nucleate boiling effects are dominant under conditions of low vapor quality, implying that the heat transfer coefficient increases with increasing heat flux as given by the predictive method of Cooper (1984) for pool boiling. In fact, Tibiriçá and Ribaski (2014) based on high-speed images of flow boiling in a quartz 400 μm I.D. tube observed active nucleation sites and bubbles departure under conditions of annular and elongated flow patterns. The behaviors displayed in Fig. 4 corroborate the predominance of nucleate boiling effects. According to this figure, the heat transfer coefficient according to both mechanisms increases with increasing heat flux. However, the increment of the heat transfer coefficient for pool boiling is steeper than for flow boiling. This behavior is explained by the fact that for flow boiling, the average vapor quality and, consequently, nucleate boiling suppression effects, increases with increasing heat flux, causing a lower increment of $\bar{h}_{TP}$ with increasing heat flux for flow boiling compared to pool boiling. Similar behaviors concerning the effect of the mass velocity on $\bar{h}_{eff}$ observed for R600a in the

present study were pointed out for R134a, R407C and R245fa in previous studies (do Nascimento et al., 2013; Leão et al., 2014, 2015).

Figures 5 and 6 present comparisons of the average effective heat transfer coefficient for the refrigerants R600a, R134a, R407C and R245fa. According to these figures, the refrigerant R600a provides the highest average effective heat transfer coefficient. By comparing Figures 5 and 6, it can be noted that, under conditions of two-phase flow along the channels and a fixed average vapor quality, the difference on the average effective heat transfer coefficient among the four fluids decreases with increasing mass velocity and liquid subcooling.

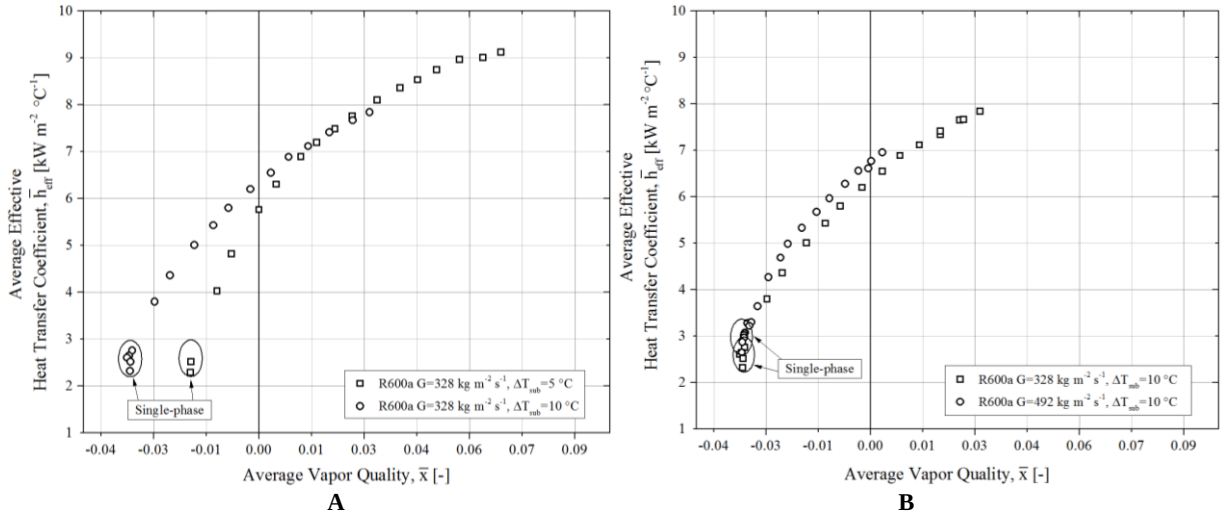


Figure 3. Illustration of (A) the effect of liquid subcooling degree and (B) mass velocity on the variation of the average effective heat transfer coefficient with average vapor quality for R600a and saturation temperature of 25 °C.

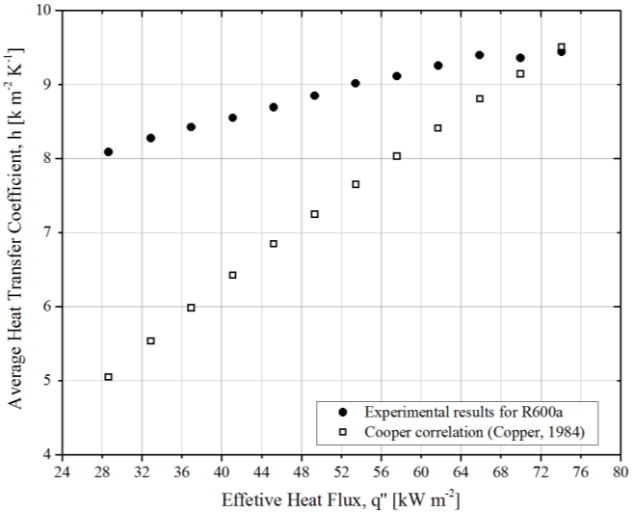


Figure 4. Comparison of the experimental average effective heat transfer coefficient for flow boiling and the heat transfer coefficient for pool boiling according to the correlation of Cooper (1984) for R600a, saturation temperature of 25 °C, liquid subcooling at the inlet plenum of 5 °C and mass velocity of 328 kg m$^{-2}$ s$^{-1}$.

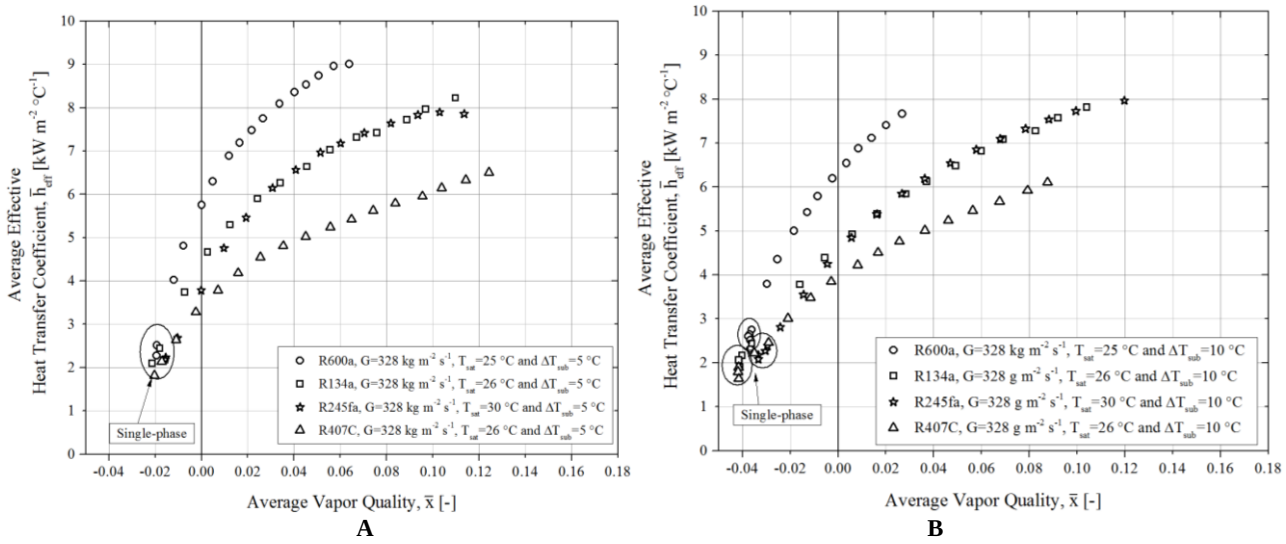


Figure 5. Illustration of the effect of fluid refrigerant on the variation of the average effective heat transfer coefficient with average vapor quality for liquid subcooling degree at the inlet plenum of (A) 5 °C and (B) 10 °C and mass velocity of 328 kg m$^{-2}$ s$^{-1}$.

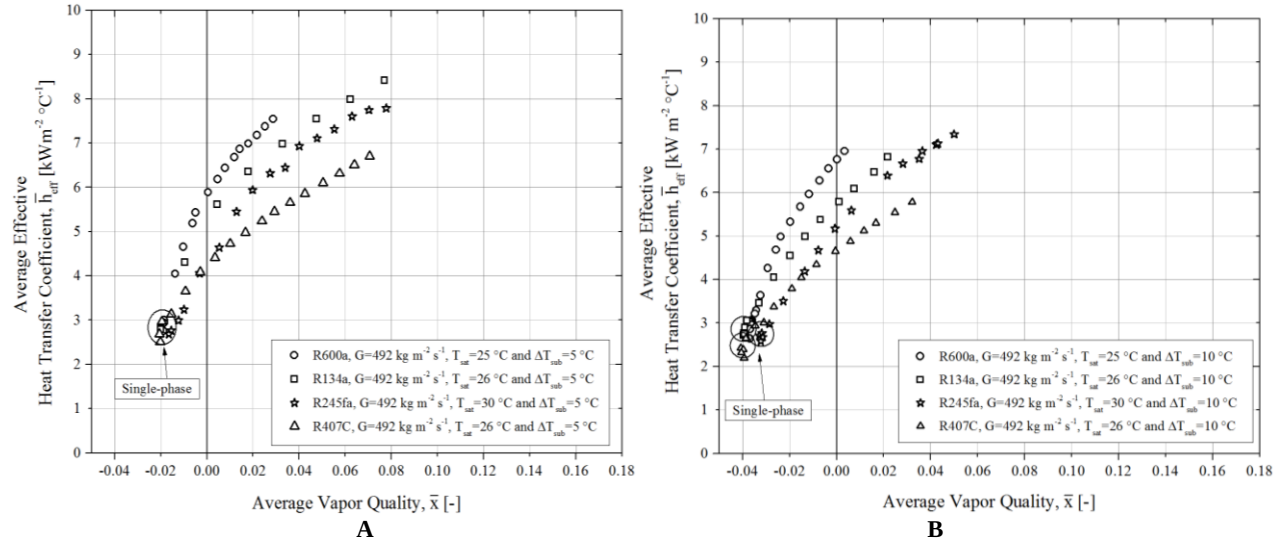


Figure 6. Illustration of the effect of fluid refrigerant on the variation of the average effective heat transfer coefficient with average vapor quality for liquid subcooling degree at the inlet plenum of (A) 5 °C and (B) 10 °C and mass velocity of 492 kg m$^{-2}$ s$^{-1}$.

## 4. CONCLUSION

New heat transfer data were obtained for R600a in a microchannels based heat spreader. Average effective heat transfer coefficients for flow boiling up to 10 kW m$^{-2}$ °C$^{-1}$ were observed. The experimental data were analyzed and the main heat transfer trends were discussed. An excess of superheating was found necessary to trigger the boiling process (onset of nucleate boiling) along the microchannels. The fluid R407C needed the lowest excess of superheating for the ONB followed by R134a, R600a and R245fa. The refrigerant R600a needed an excess of superheating of 12.4 °C corresponding a value 3.3 times higher than R134a. The Kandlikar et al. (2006) method provided reasonable predictions of the ONB. Under the presence of flow boiling mechanism along the microchannels, the average effective heat transfer coefficient increases with increasing the mass velocity and the liquid subcooling. Under flow boiling conditions and a fixed value of $\bar{x}$, the refrigerant R600a provided the highest average effective heat transfer coefficient. Finally, despite of its higher excess of superheating for the ONB, it can be concluded based on the results described in the present study, that the refrigerant R600a presents a reasonable potential to be used in heat sinks based on flow boiling through microchannels due to its low saturation pressure, satisfactory heat transfer performance, almost negligible refrigerant charge, and low global warming and ozone depletion potentials.

## 5. ACKNOWLEDGEMENTS

The authors gratefully acknowledge the scholarships to the first author and the financial supports given by CNPq (National Council of Scientific and Technological Development, Brazil) and CAPES (Coordination for the Improvement of Higher Level -or Education- Personnel, Brazil). The first author acknowledges also the support given by IF Goiano -campus Rio Verde.

## 6. REFERENCES

Abernethy, R.B. and Thompson, J.W., 1973. *Handbook uncertainty in gas turbine measurements*. Center, Arnold Engineering Development, Tennessee.

Agostini, B., Fabbri, M., Park, J.E., Wojtan, L., Thome, J.R. and Michel, B., 2007. "State of the Art of High Heat Flux Cooling Technologies". *Heat Transf. Eng.*, Vol. 28, p. 258–281.

Agostini, B. and Thome, J.R., 2005. "Comparison of an extended database of flow boiling heat transfer coefficients in multi-microchannel elements with the three-zone model". In: ECI *International Conference on Heat Transfer and Fluid Flow in Microscale*. Castelvecchio Pascoli, Italy, pp. 25–30.

Awad, M.M., Muzychka, Y.S., 2008. "Effective property models for homogeneous two-phase flows". *Exp. Therm. Fluid Sci.*, Vol. 33, p. 106–113.

Bergles, A.E. and Rohsenow, W.M., 1964. "The Determination of Forced-Convection Surface-Boiling Heat Transfer". *J. Heat Transfer*, Vol. 86, p. 365–372.

Bertsch, S.S., Groll, E.A. and Garimella, S. V., 2008. "Refrigerant flow boiling heat transfer in parallel microchannels as a function of local vapor quality". *Int. J. Heat Mass Transf.*, Vol. 51, p. 4775–4787.

Chávez, C.A., Leão, H.L.S.L. and Ribatski, G., 2014. "A critical review on thermal instabilities in multi-microchannels heat sinks due to confined bubble growth". In: *15th Brazilian Congress of Thermal Sciences and Engineering*. Belém, Brazil.

Chen, J.C., 1966. "Correlation for boiling heat transfer to saturated fluids in convective flow". *Ind. Eng. Chem. Process Des. Dev.*, Vol. 5, p. 322–329.

Chen, T. and Garimella, S. V., 2006. "Measurements and high-speed visualizations of flow boiling of a dielectric fluid in a silicon microchannel heat sink". *Int. J. Multiph. Flow*, Vol. 32, p. 957–971.

Chen, Y., Groll, M., Mertz, R. and Kulenovic, R., 2005. "Pool boiling heat transfer of propane, isobutane and their mixtures on enhanced tubes with reentrant channels". *Int. J. Heat Mass Transf.*, Vol. 48, p. 2310–2322.

Cioncolini, A. and Thome, J.R., 2011. "Algebraic turbulence modeling in adiabatic and evaporating annular two-phase flow". *Int. J. Heat Fluid Flow*, Vol. 32, p. 805–817.

Colgan, E.G., Furman, B., Gaynes, M., Graham, W.S., LaBianca, N.C., Magerlein, J.H., Polastre, R.J., Rothwell, M.B., Bezama, R.J., Choudhary, R., Marston, K.C., Toy, H., Wakil, J., Zitz, J.A. and Schmidt, R.R., 2007. "A practical implementation of silicon microchannel coolers for high power chips". *IEEE Trans. Components Packag. Technol.*, Vol. 30, p. 218–225.

Collier, J.G. and Thome, J.R., 1994. *Convective Boiling and Condensation*. Clarendon Press.

Cooper, M.G., 1984. "Heat Flow Rates in Saturated Nucleate Pool Boiling-A Wide-Ranging Examination Using Reduced Properties". *Adv. Heat Transf.*, Vol. 16, p. 157–239.

Daniels, B.J., Liburdy, J.A. and Pence, D.V., 2011. "Experimental studies of adiabatic flow boiling in fractal-like branching microchannels". *Exp. Therm. Fluid Sci.*, Vol. 35, p. 1–10.

Davis, E.J. and Anderson, G.H., 1966. "The incipience of nucleate boiling in forced convection flow". *AIChE J.*, Vol. 12, p. 774–780.

do Nascimento, F.J., Leão, H.L.S.L. and Ribatski, G., 2013. "An experimental study on flow boiling heat transfer of R134a in a microchannel-based heat sink". *Exp. Therm. Fluid Sci.*, Vol. 45, p. 117–127.

Harirchian, T. and Garimella, S. V., 2009. "Effects of channel dimension, heat flux, and mass flux on flow boiling regimes in microchannels". *Int. J. Multiph. Flow*, Vol. 35, p. 349–362.

Hetsroni, G., Mosyak, A., Segal, Z. and Ziskind, G., 2002. "A uniform temperature heat sink for cooling of electronic devices". *Int. J. Heat Mass Transf.*, Vol. 45, p. 3275–3286.

Kaew-On, J., Sakamatapan, K. and Wongwises, S., 2011. "Flow boiling heat transfer of R134a in the multiport minichannel heat exchangers". *Exp. Therm. Fluid Sci.*, Vol. 35, p. 364–374.

Kaew-On, J. and Wongwises, S., 2009. "Experimental investigation of evaporation heat transfer coefficient and pressure drop of R-410A in a multiport mini-channel". *Int. J. Refrig.*, Vol. 32, p. 124–137.

Kandlikar, S.G., Garimella, S., Li, D., Colin, S. and King, M.R., 2006. *Heat Transfer and Fluid Flow in Minichannels and Microchannels*. Elsevier Science, 1st edition.

Kanizawa, F.T., Tibiriçá, C.B. and Ribatski, G., 2016. "Heat transfer during convective boiling inside microchannels". *Int. J. Heat Mass Transf.*, Vol. 93, p. 566–583.

Kew, P. a. and Cornwell, K., 1997. "Correlations for the prediction of boiling heat transfer in small-diameter channels". *Appl. Therm. Eng.*, Vol. 17, p. 705–715.

Leão, H.L.S.L., Chávez, C.A., do Nascimento and F.J., Ribatski, G., 2015. "An analysis of the effect of the footprint orientation on the thermal-hydraulic performance of a microchannels heat sink during flow boiling of R245fa". *Appl. Therm. Eng.*, Vol. 90, p. 907–926.

Leão, H.L.S.L., do Nascimento, F.J. and Ribatski, G., 2014. "Flow boiling heat transfer of R407C in a microchannels based heat spreader". *Exp. Therm. Fluid Sci.*, Vol. 59, p. 140–151.

Levy, F.L., 1981. "A modified Maxwell-Eucken equation for calculating the thermal conductivity of two-component solutions or mixtures". *Int. J. Refrig.*, Vol. 4, p. 223–225.

Li, W. and Wu, Z., 2010. "A general correlation for evaporative heat transfer in micro/mini-channels". *Int. J. Heat Mass Transf.*, Vol. 53, p. 1778–1787.

Moffat, R.J., 1988. "Describing the uncertainties in experimental results". *Exp. Therm. Fluid Sci*., Vol. 1, p. 3–17.

Park, J.E. and Thome, J.R., 2010. "Critical heat flux in multi-microchannel copper elements with low pressure refrigerants". *Int. J. Heat Mass Transf.*, Vol. 53, p. 110–122.

Ribatski, G., 2013. "A Critical Overview on the Recent Literature Concerning Flow Boiling and Two-Phase Flows Inside Micro-Scale Channels". *Exp. Heat Transf.*, Vol. 26, p. 198–246.

Sempértegui-Tapia, D. and Ribatski, G., 2013. "An analysis of experimental data and prediction methods for heat transfer coefficient during convective boiling in non-circular micro-scale channels". In: *8th International Conference on Multiphase Flow*. Jeju, Korean.

Shah, R.K. and London, A.L., 1978. *Laminar Flow Forced Convection in Ducts*. New York: Eds. Irvine, T. E and Hartnett, J. P., Academic Press.

Stephan, K. and Preußer, P., 1979. "Wärmeübergang und maximale Wärmestromdichte beim Behältersieden binärer und ternärer Flüssigkeitsgemische". *Chemie Ing. Tech.*, Vol. 51, p. 37.

Szczukiewicz, S., Magnini, M. and Thome, J.R., 2014. "Proposed models, ongoing experiments, and latest numerical simulations of microchannel two-phase flow boiling". *Int. J. Multiph. Flow*, Vol. 59, p. 84–101.

Thome, J.R., 1996. "Boiling of new refrigerants: a state-of-the-art review". *Int. J. Refrig.*, Vol. 19, p. 435–457.

Tibiriçá, C.B. and Ribatski, G., 2013. "Flow boiling in micro-scale channels-Synthesized literature review". in: *International Journal of Refrigeration*. p. 301–324.

Tibiriçá, C.B. and Ribatski, G., 2014. "Flow patterns and bubble departure fundamental characteristics during flow boiling in microscale channels". *Experimental Thermal and Fluid Science*, Vol. 59, p. 152-165.

Tuckerman, D.B. and Pease, R.F.W., 1981. "High-performance heat sinking for VLSI". *IEEE Electron Device Lett.*, Vol. 2, p. 126–129.

Wang, G., Cheng, P. and Bergles, A.E., 2008. "Effects of inlet/outlet configurations on flow boiling instability in parallel microchannels". *Int. J. Heat Mass Transf.*, Vol. 51, p. 2267–2281.

Xu, J., Shen, S., Gan, Y., Li, Y., Zhang, W. and Su, Q., 2005. "Transient flow pattern based microscale boiling heat transfer mechanisms". *J. Micromechanics Microengineering*, Vol. 15, p. 1344–1361.

Zhang, H.Y., 2005. "Flow boiling heat transfer in microchannel heat sinks of different flow orientations", in: *Proceedings of the ASME Summer Heat Transfer Conference*. San Francisco, USA.

## 7. RESPONSIBILITY NOTICE

The author(s) is (are) the only responsible for the printed material included in this paper.